RSC Advances

PAPER

Cite this: *RSC Adv.*, 2016, **6**, 79275

Removal of metformin hydrochloride by *Alternanthera philoxeroides* biomass derived porous carbon materials treated with hydrogen peroxide†

Xixian Huang,[ab] Yunguo Liu,*[ab] Shaobo Liu,*[cd] Zhongwu Li,[ab] Xiaofei Tan,[ab] Yang Ding,[ab] Guangming Zeng,[ab] Yan Xu,[ab] Wei Zeng[ab] and Bohong Zheng[c]

Received 1st April 2016
Accepted 16th August 2016

DOI: 10.1039/c6ra08365j

www.rsc.org/advances

Hydrogen peroxide modified biochar (mBC) derived from *Alternanthera philoxeroides* (AP) biomass was used to investigate the adsorption properties of metformin hydrochloride (MF). Additionally, the effects of pH and Cu(II) on MF adsorption were also evaluated. Adsorption kinetics and isotherms indicated that the adsorption process of MF on mBC was fitted better to the pseudo-second-order model and Freundlich model, respectively. The adsorption thermodynamic analysis revealed that the adsorption processes of MF were spontaneous and endothermic. In this study, there was a great influence of pH on MF adsorption capacity related to the various species of MF (cationic, zwitterionic and anionic) at different pH. Furthermore, it could be found that the presence of Cu(II) facilitated MF adsorption in the range of pH 3.0–7.0, while the adsorption capacity of MF decreased with the increase of Cu(II) concentration. At pH < 3 or pH > 7, the presence of Cu(II) had only minor effects on MF adsorption.

1. Introduction

Diabetes mellitus is threatening more and more people's health, this is a group of metabolic diseases characterized by hyperglycemia resulting from defects in insulin secretion, insulin action, or both.[1] Metformin is an antihyperglycemic agent and it can lower the blood glucose concentration without causing hypoglycemia.[2] However, metformin potentially causes harm to humans and animals in the natural environment. Metformin could cause adverse effects on gastrointestinal and lactic acidosis, which is rare but potentially fatal.[2] The widely prescribed anti-diabetic metformin is among the most abundant pharmaceuticals found in effluent and is structurally dissimilar from hormones.[3] It was reported that a certain concentration of metformin in wastewater effluent could cause various damage to fathead minnows (*Pimephales promelas*), including the development of intersex gonads in males, male fish size reduction, and fecundity reduction. Furthermore, juvenile fathead minnows were more susceptible to the estrogenic effects of metformin during a 7 day exposure than older and sexually mature male fathead minnows.[4] Besides, some studies demonstrated that the exposure of adult fathead minnows (including exposure during the critical period of male sexual development) to metformin can result in severe endocrine impacts such as intersex.[5,6] Therefore, metformin acts as an endocrine disruptor at environmentally relevant concentrations.

Recent studies of watersheds downstream of wastewater treatment plants (WWTPs) showed that anti-diabetic drug metformin is one of the most abundant pharmaceuticals, which was thought to be mostly deposited into the aquatic environment by mass[7] and detected in effluent at concentrations ranging from 1 to 47 μg L^{-1}.[7–9] Although largely converted to byproducts in WWTPs, the biguanidine drug is excreted in patient's waste in its active form and is still deposited into the environment in a relatively high amount for a pharmaceutical, at up to 6 tons per year from individual WWTPs in urban areas.[10] Thus, it is inevitable to study the adsorption properties of metformin onto adsorbents in aqueous solutions.

Biochar contains porous carbonaceous structure and an array of functional groups, which is the by-product of biomass pyrolysis under a negligible or limited supply of oxygen.[11,12] Various types of biomass including wood waste, crop residues, and dairy manure have been used to produce biochars.[13,14] For

[a]*College of Environmental Science and Engineering, Hunan University, Changsha 410082, PR China. E-mail: hnliuyunguo@163.com; Fax: +86 731 88822829; Tel: +86 731 88649208*

[b]*Key Laboratory of Environmental Biology and Pollution Control (Hunan University), Ministry of Education, Changsha 410082, PR China*

[c]*School of Architecture and Art Central South University, Central South University, Changsha 410082, P. R. China. E-mail: liushaobo23@aliyun.com; Fax: +86 731 88710171; Tel: +86 731 88830923*

[d]*School of Metallurgy and Environmental, Central South University, Changsha 410083, P.R. China*

† Electronic supplementary information (ESI) available. See DOI: 10.1039/c6ra08365j

instance, biochars derived from soybean stover and peanut shell had strong affinities for trichloroethylene adsorption.[15] Similarly, biochar made from agricultural biomass waste exhibited a high adsorption capacity on organic pollutants.[16] However, the studies of antidiabetic drugs adsorption by biochar was very scarce, especially metformin hydrochloride.

As one of the high-level nutrient adapted hydrophytes, *Alternanthera philoxeroides* (AP) has been widely used in the ecological restoration of eutrophic lakes.[17] However, the large amount of AP brings additional problems which need to be handled.[18] Currently, AP waste is often disposed by natural decomposition, which could cause secondary environmental problems by releasing pathogens and methane.[18] Therefore, using AP as a source material for biochar production may be eco-friendly and cost-effective. In addition, the increases of oxygen-containing surface functional groups and surface area of biochar could enhance the adsorption capacity of pollutants.[15] Thus, we applied that H_2O_2, as a strong oxidant to improve the adsorption performance of biochar.

Recently, the medicinal uses and applications of metals and metal complexes are of increasing clinical and commercial importance. The metal-drug complexes can be used to change human abdominal environment. Copper complex is one of the important metal complexes, which could cause environmental pollution.[19,20] Moreover, metallic elements play a crucial role in living systems.[21] Metals are easily losing electrons from the elemental or metallic state to form positively charged ions which tend to be soluble in biological fluids. Metal ions are electron deficient and most biological molecules are electron rich. Therefore, these opposing charges attract each other, which may lead to the general tendency of metal ions to bind to and interact with biological molecules.[20] Several studies have indicated that the formation of complexes between metallic ions and organic pollutants would affect the adsorption efficiency of adsorbents. For example, the presence of metallic ions (Ca^{2+}, Mg^{2+} and Na^{+}) greatly influenced the sorption of tetracyclines (TC) in soils or mineral constituents, due to the formation of complexes between metallic ions and TC.[22] Similarly, the coexistence of TC and Cu(II) could enhance the adsorption of TC on montmorillonite.[23] Furthermore, the complexes of TC and Cu(II) existed as various species (CuH_2L^{2+}, $CuHL^{+}$, and CuL) at different solution pH, which had higher adsorption coefficients compared with TC (H_3L^{+}, H_2L, and HL^{-}).[24] Thus, heavy metal in the natural environment could affect the transport and fate of organic pollutants. In addition, the complexation reaction between organic pollutant and heavy metal at various solution pH values results in different specific species. Therefore, it is necessary to investigate the effects of pH and the presence of heavy metal on the adsorption of pollutants on natural sorbents.

In this study, AP was used to prepare biochar *via* slow pyrolysis at 300 °C, and the resulted biochar was modified by H_2O_2. The modified biochar was applied to determine the adsorption behavior of MF. To our knowledge, few studies have focused on the adsorption behavior of MF on biochar, and the effects of pH and Cu(II) on MF adsorption onto biochar remain unknown. Hence, the specific objectives of this study were to (1) compare physical and chemical properties of H_2O_2-modified and unmodified biochar, and the adsorption capacity of MF on H_2O_2-modified and unmodified biochar; (2) examine isotherms, kinetics and thermodynamic properties of MF sorption onto mBC; (3) explore the adsorption of MF on mBC as affected by pH and Cu(II).

2. Materials and methods

2.1 Biochar preparation

The AP used for biochar production was collected from Changsha, Hunan province, China. AP was washed with ultrapure water to remove the attached dust, and then dried at 80 °C for 24 h. Then, the dried biomass were pyrolyzed in a lab-scale tubular reactor (SK-G08123K, China) at 300 °C and 450 °C, respectively at a heating rate of 5 °C min^{-1}, in N_2 environment for 2 h. The biochar samples (BC) were then cooled at room temperature. BC were ground through a 0.15 mm sieve for this study. The final BC sample was stored for later experiments.

To make the mBC, about 5 g of the final BC sample was placed into 50 mL 15% H_2O_2 solution. Then the mixture was ultrasonic dispersion for 2 h. The suspension was vibrated in oscillator for 5 h at 25 °C, and then rinsed with ultrapure water and dried at 80 °C. The resulted mBC was stored for later experiments.

2.2 Biochar characterization

The elemental composition on the sample surface was determined using an ESCALAB 250Xi X-ray Photoelectron Spectrometer (XPS) (Thermo Fisher, USA). Carbon, hydrogen and nitrogen contents of the samples were determined using a CHN Elemental Analyzer (Elementar Vario El Cube, Germany). Brunauer, Emmett and Teller (BET) surface area was determined using a gas sorption analyzer (Quantachrome Quadrasorb SI, USA) and the total pore volume was examined from the N_2 adsorption–desorption isotherms. Fourier transform infra-red spectrophotometer (FTIR) (Nicolet Magna-IR 750, USA) was used to measure the functional groups of sample's surface. The pH of the point of zero charge (pH_{pzc}) was measured using electroacoustic spectrometer (ZEN3600 Zetasizer, UK) by adding 0.1 g mBC to solution with pH ranging from 1.0 to 12.0.

2.3 Batch adsorption

Ultrapure water with a resistivity of 18.25 MΩ cm^{-1} was used in this study. The concentrations of MF (0.05–3.2 mmol L^{-1}) were prepared by dissolving analytic grade metformin hydrochloride into ultrapure water.

The impact of pH on mBC adsorption was examined by adjusting the initial MF solutions (0.5 mmol L^{-1}) ranging from 1.0 to 12.0 with 1 M NaOH or 1 M HCl. The influence of Cu on mBC adsorption was conducted by adding Cu^{2+} (0.1, 0.5, and 1 mmol L^{-1}) into MF solutions. Adsorption kinetic was conducted by adding 0.1 g mBC into 50 mL of the 0.5 mmol L^{-1} solutions. These suspensions were shaken at 160 rpm at 25 °C for the designated time periods. Experiments for adsorption isotherms were conducted at the initial concentrations of MF (0.05, 0.1,

0.2, 0.5, 0.8, 1.6, 2.4 and 3.6 mmol L^{-1}) and the shaking period of 24 h. Thermodynamic data were obtained at the temperature of 25, 35 and 45 °C based on the experiments of adsorption isotherms. The influence of background ionic strength on MF adsorption was determined at appropriate pH with the addition of different concentrations of NaCl and $CaCl_2$ (0, 0.1, 0.2, 0.4, 0.8 and 1.0 mmol L^{-1}). The mBC with 0.1 g was added into each solution, and suspensions were shaken at 160 rpm under 25 °C for 24 h.

2.4 Desorption experiment

The regeneration study was conducted by using hydrochloric acid as stripping agent. The mBC which has been used to adsorb MF (2.4 mmol L^{-1}) was added into 50 mL of 0.5 mol L^{-1} HCl solution, shaken at 160 rpm under 25 °C for 10 h. Then the adsorbent was washed to neutral by deionized water and collected to reuse.

2.5 MF detection

The concentration of solute in supernatant solution was measured by high performance liquid chromatography (Agilent 1200, USA) equipped with C18 column with column temperature at 25 °C. The mobile phase consisted of acetonitrile (65%) and 10 mM monopotassium phosphate (35%) at a flow rate of 1.0 mL min^{-1}. The pH of phosphate buffer was adjusted to 5.75 with *o*-phosphoric acid which was filtered through 0.2 μm filter. MF was analyzed by a UV detector at 233 nm. The calibration curve was linear in the concentration range of 0.01–0.1 mmol L^{-1}.

3. Results and discussion

3.1 Characteristics of biochar

The BET characteristics of BC and mBC were presented in Table 1. The BET surface area of BC increased (from 42.75 to 85.68 m^2 g^{-1}) with the increase of pyrolysis temperature (from 300 to 450 °C). Moreover, the BET surface area of mBC produced at 450 °C was 178.37 m^2 g^{-1}, which was higher than that of BC (85.68 m^2 g^{-1}). These results indicated that the surface area of BC increased obviously by increasing pyrolysis temperature and H_2O_2 modification.

As shown in Table 2, the CHN analysis indicated similar hydrogen and nitrogen contents of BC and mBC. However, the carbon content of mBC (43.47%) was lower than that of BC (54.93%), suggesting that part of the carbon in BC was oxidized by the H_2O_2 resulting in the calculated higher oxygen content of the mBC (49.87%) than that of BC (36.42%). The surface chemical elements of biochar before and after modification or adsorption were determined by XPS. The XPS survey spectra (Fig. 1) indicated that the main elements of mBC made at 300 °C were carbon (75.21%), oxygen (20.34%) and nitrogen (4.45%), and the contents of these elements changed to 75.57%, 19.36% and 5.07% after MF adsorption, respectively. Moreover, the main elements of mBC after MF adsorption in the presence of Cu(II) were carbon (75.78%), oxygen (18.51%), nitrogen (5.09%), and copper (0.63%). These changes of element content among three biochars indicated that the presence of MF and/or Cu(II) may influence the element content, which could be attributed to the adsorption of MF onto biochar. As shown in Fig. 2, the peaks observed at binding energy of 283.7, 285.4, 286.5 and 287.8 eV for three carbon materials correspond to C–C, C–N, C–O and C=O, respectively. A new peak of mBC at 288.9 eV could be assigned to –COO–.[25] Therefore, these results indicated that mBC was functionalized well with –COO– groups through H_2O_2 treatment.

Table 2 Bulk elemental composition of biochars made at 300 °C

	C (%)	H (%)	O[a] (%)	N (%)	H/C	O/C	N/C
BC	54.93	4.66	36.42	3.99	1.02	0.50	0.06
mBC	43.47	3.66	49.78	3.09	1.01	0.86	0.06

[a] Determined by weight difference assuming that the total weight of the samples was made up of the tested elements only.

The FTIR spectra of BC and mBC produced at 300 °C are shown in Fig. S1.† Characteristic peak at about 3420 cm^{-1} was related to the stretching vibration of –OH groups. The band at 3155.2 cm^{-1} may be mainly due to the stretching vibration of –NH containing in Cu(II)-$(MF)_2$.[20] The peak at 2927.5 cm^{-1} was connected with asymmetrical stretching vibration of methylene groups and the peak at 2356.6 cm^{-1} could correspond to C≡C in-line deformation vibration or carbon dioxide.[26] The band near at 1623.8 cm^{-1} was assigned to the stretching vibration of –OH deformation of water and C=O stretching vibrations of ester.[27] The peak near at 1430 cm^{-1} may be attributed to the –COO– groups and the band near at 780 cm^{-1} was related to carboxylate (–COO–) deviational vibration and symmetric stretching.[28]

The FTIR spectra of BC (Fig. S1a†) and mBC (Fig. S1b†) revealed that the band at 1430.9 cm^{-1} shifted to the higher wavenumbers (1434.8 cm^{-1}) after modification, which demonstrated that H_2O_2 treatment could influence the oxygen-

Table 1 BET characteristics of biochar (BC) and H_2O_2-modified biochar (mBC) produced from AP

Adsorbent	Pyrolysis temperature (°C)	BET surface area (m^2 g^{-1})	Pore volume (cm^3 g^{-1})	Average pore (nm)
Biochar	300	42.75	0.05786	4.962
	450	85.68	0.07358	5.384
H_2O_2-modified biochar	300	114.91	0.09962	5.867
	450	178.37	0.13240	5.952

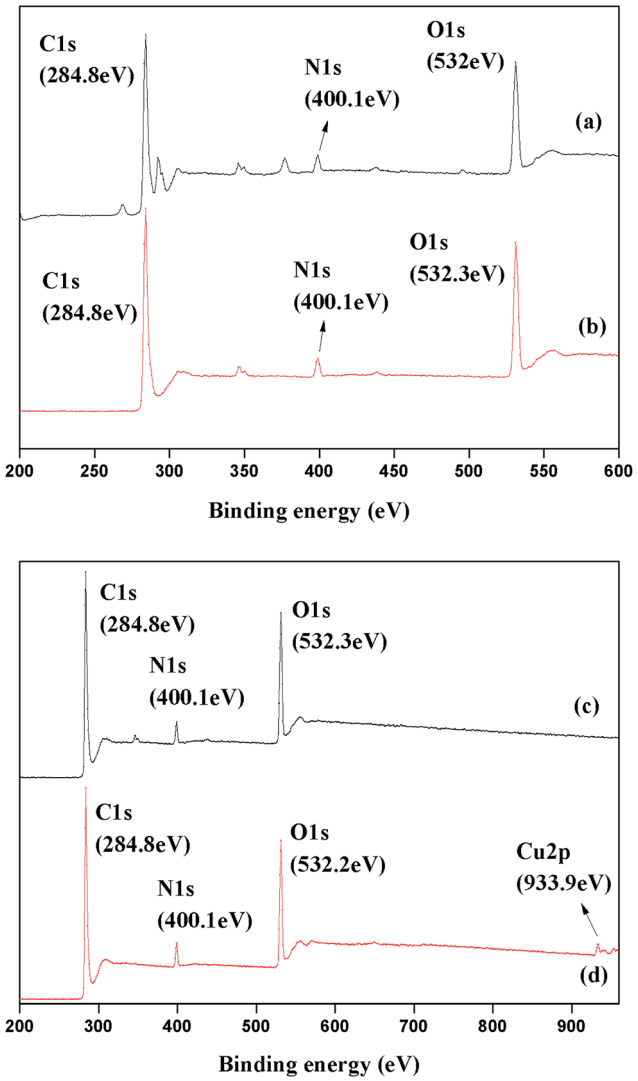

Fig. 1 XPS survey spectra of (a) pristine biochar (BC), (b) H_2O_2-modified biochar (mBC), (c) metformin hydrochloride (MF) adsorption on mBC, and (d) MF and Cu(II) adsorption on mBC (biochar: 300 °C).

containing functional groups of biochar surface.[29,30] Compared to the FTIR spectra of mBC (Fig. S1b†), the peak of mBC after MF adsorption (Fig. S1c†) at 1434.8 cm^{-1} and 782.9 cm^{-1} were shifted to 1438.7 cm^{-1} and 779.1 cm^{-1}, respectively, which may indicate that –COO– groups on mBC was contributed to the MF adsorption. In addition, the FTIR spectra of mBC after MF adsorption in the presence of Cu(II) (Fig. S1d†) showed that those peaks, such as –CO, –OH, and –COO–, had changes compared to other spectrums. The possible explanation may be that the existence of Cu(II) could influence the adsorption process of MF on mBC. Moreover, the appearance of the new band at 3155.2 cm^{-1} may indicate that a part of MF was adsorbed at the form of Cu(II)–$(MF)_2$ by mBC.[20]

3.2 Kinetic studies

Pseudo-first-order, pseudo-second-order, and intra-particle diffusion were used to simulate the kinetic of MF sorption on mBC made at 300 and 450 °C. Governing equations for these models can be written as:[31,32]

$$\text{First-order}: q_t = q_e\left(1 - e^{k_1 t}\right) \quad (1)$$

$$\text{Second-order}: q_t = \frac{k_2 q_e^{\,2} t}{1 + k_2 q_e t} \quad (2)$$

$$\text{Intra-particle diffusion}: q_t = k_{pi} t^{1/2} + C \quad (3)$$

where q_t (μmol g^{-1}) and q_e (μmol g^{-1}) are the amount of sorbate removed at time t and at equilibrium, respectively, and k_1 (min) and k_2 (g μmol^{-1} min^{-1}) are the first-order and second order sorption rate constants, respectively. The k_{pi} (μmol g^{-1} $min^{-1/2}$) is the diffusion rate constant of intra-particle. C is the intercept related to the thickness of the boundary layer.

The relative parameters calculated from pseudo-first-order model, pseudo-second-order model and intra-particle diffusion model are listed in Table 3. The correlation coefficient (R^2) of the pseudo-second-order model (0.98 and 0.96) was higher than those of the pseudo-first-order model (0.94 and 0.89), indicating the experimental data fitted better to pseudo-second-order model. The values of q_e calculated from pseudo-second-order model (120.81 and 145.65 μmol g^{-1}) were more fitted in the experimental value (122 and 153 μmol g^{-1}). The pseudo-second-order model supposes that the sorption rate of MF is controlled by chemisorption involving valence forces through the sharing or exchange of electrons between mBC surface and MF.[33] Furthermore, as shown in Fig. 3, MF adsorption on mBC at the beginning 8 h was rapidly and the adsorption capacities were 104 and 132 μmol g^{-1} for mBC pyrolyzed under 300 °C and 450 °C, respectively.

The intra-particle diffusion model indicated that the adsorption process could be divided into three steps, including the diffusion of adsorbate through the bulk solution to the external surface of biochar, MF pass through the liquid film to the biochar surface, and MF interactions with the surface atoms of the biochar.[34] The adsorption rate became slower with the adsorption process by comparing the values of k_{pi}, especially at final steps (Table 3). The potential explanations may be attributed to the following factors: (1) the enhanced electrostatic repulsion between the mBC surface and the MF; (2) the lower driving force resulting from the lower MF concentration; and (3) the smaller pores on mBC surface for diffusion.[35,36]

3.3 Adsorption isotherms

Langmuir, Freundlich and Temkin adsorption models were used to fit the MF adsorption isotherm data.[37] Governing equations for these models can be written as:

$$\text{Langmuir model}: q_e = \frac{q_{max} K_L C_e}{1 + K_L C_e} \quad (4)$$

$$\text{Freundlich model}: q_e = K_F C_e^{\,1/n} \quad (5)$$

$$\text{Temkin model}: q_e = \frac{RT}{b_T} \ln A_T + \frac{RT}{b_T} \ln C_e \quad (6)$$

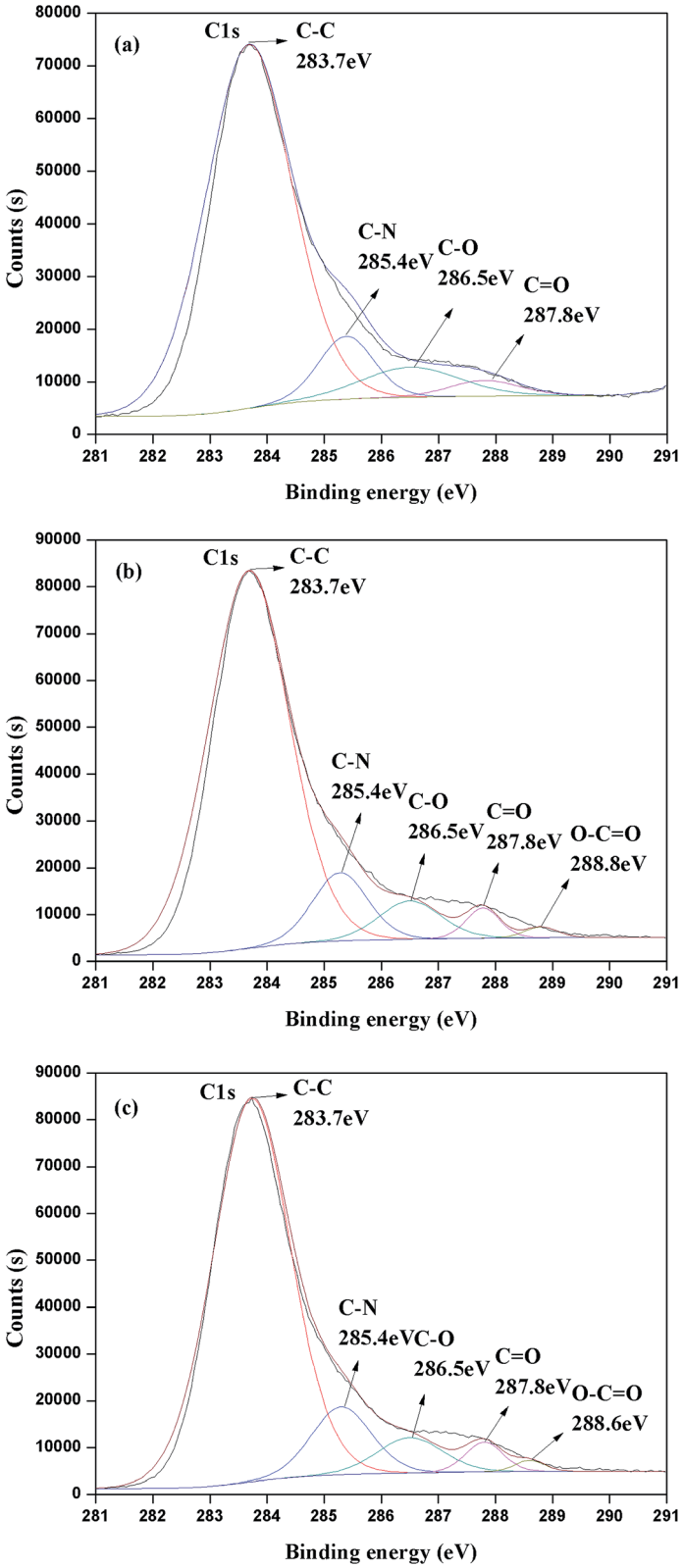

Fig. 2 C 1s XPS spectra of (a) pristine biochar (BC), (b) H_2O_2-modified bicoahr (mBC), and (c) mBC after metformin hydrochloride (MF) adsorption (biochar: 300 °C).

where K_L and K_F are the Langmuir bonding term related to interaction energies (L μmol^{-1}) and the Freundlich affinity coefficient ((μmol g^{-1}) (μmol L^{-1})$^{-n}$), respectively. A_T is the Tempkin isotherm equilibrium binding constant (L g^{-1}), and b_T is Tempkin isotherm constant. R is the universal gas constant (8.314 J mol^{-1} K^{-1}), and T is absolute temperature (K). The C_e is

Table 3 Pseudo-first-order and pseudo-second-order model parameters for metformin hydrochloride (MF) sorption on H_2O_2-modified biochar (mBC) (300 °C) at 25 °C

	Parameters		
Kinetic models	Units	300 °C	450 °C
Pseudo-first-order parameters	K_1 (min^{-1})	9.57×10^{-3}	1.77×10^{-2}
	q_e (μmol g^{-1})	111.44	136.77
	R^2	0.94	0.89
Pseudo-second-order parameters	K_2 (g μmol^{-1} min^{-1})	1.14×10^{-4}	1.76×10^{-4}
	q_e (μmol g^{-1})	120.81	145.65
	R^2	0.98	0.96
Intra-particle diffusion parameters	k_{p_1} (μmol g^{-1} $min^{-1/2}$)	6.37	5.52
	C_1	3.89	38.57
	R_1^2	0.97	0.98
	k_{p_2} (μmol g^{-1} $min^{-1/2}$)	1.66	1.98
	C_2	63.61	85.57
	R_2^2	0.92	0.93
	k_{p_3} (μmol g^{-1} $min^{-1/2}$)	0.32	0.36
	C_3	104.47	132.91
	R_3^2	0.98	0.97

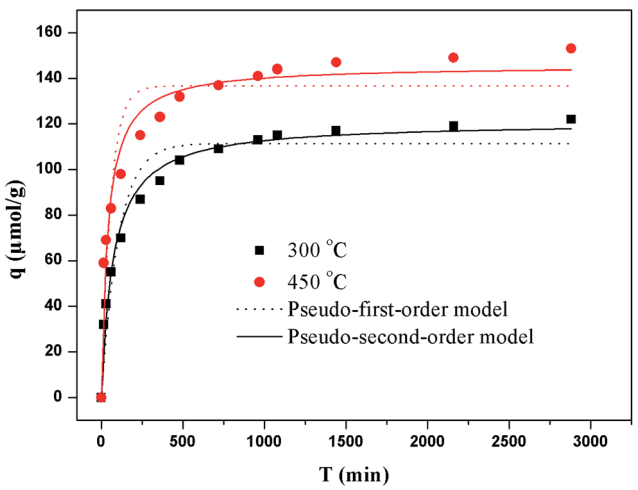

Fig. 3 Pseudo-first-order sorption kinetics and pseudo-second-order sorption kinetics for MF adsorption onto mBC (initial MF concentration: 0.5 mmol L^{-1}; pH: 3.0; reaction temperature: 25 °C).

the equilibrium concentration (μmol L^{-1}), q_e is the amount of MF adsorbed at equilibrium (μmol g^{-1}), q_{max} is the maximum adsorption capacity of the solute (μmol g^{-1}). The n is the Freundlich linearity constant related to the surface site heterogeneity. The adsorption represents favorable adsorption condition if n is greater than 1 and less than 10 ($1 < n < 10$). The Langmuir model assumes monolayer adsorption onto a homogeneous surface with no interactions between the adsorbed molecules. The Freundlich model is an empirical equation commonly used for heterogeneous surfaces. The Temkin model contains a factor that explicitly taking into account of adsorbent–adsorbate interactions and its derivation is characterized by a uniform distribution of binding energies (up to some maximum binding energy).

The MF adsorption isotherms on mBC at three temperatures are shown in Fig. 4. As shown in Table 4, the correlation coefficient (R^2) values of Freundlich model (0.99, 0.99, 0.99 and 0.99, 0.99, 0.99) were higher than those of Langmuir model (0.97, 0.96, 0.95 and 0.97, 0.97, 0.96) and Temkin model (0.88, 0.86, 0.85 and 0.85, 0.83, 0.84). Therefore, these adsorption data of MF onto mBC fitted Freundlich model better than Langmuir model and Temkin model, indicating that the heterogeneity adsorption of the MF to the bonding sites could be attributed to the surface functional groups of mBC.[37] Moreover, the constants n of Freundlich model at three temperatures were 1.89, 1.99, 2.35 and 1.92, 2.01, 2.27, respectively.

Fig. 5 shows the adsorption capacity of MF on BC and mBC at equilibrium. It demonstrated that the adsorption amount of biochar modified by H_2O_2 (258 μmol g^{-1} for 300 °C and 335.5 μmol g^{-1} for 450 °C) was higher than that of unmodified biochar (226 μmol g^{-1} for 300 °C and 248.5 μmol g^{-1} for 450 °C). The XPS, FTIR and BET studies indicated that several reasons may be responsible for the increasing adsorption capacity: (1) mBC was functionalized well with –COO– groups comparing with BC, which may be contributed to the MF adsorption; (2) compared to BC, mBC had a higher surface area contained more binding sites, which may be related to the MF adsorption; (3) the surface area increase with the increase of pyrolysis temperature.

3.4 Adsorption thermodynamic analysis

The thermodynamic data, such as Gibbs free energy ΔG^0, enthalpy ΔH^0, entropy ΔS^0, can be calculated using the following equations:

$$\Delta G^0 = -RT \ln K_e \quad (7)$$

$$\ln K_e = \frac{\Delta S^0}{R} - \frac{\Delta H^0}{RT} \quad (8)$$

where ΔG^0 is the stand free energy change of the ion exchange (kJ mol^{-1}), ΔH^0 (kJ mol^{-1}) is the enthalpy change, ΔS^0 (J mol^{-1} K^{-1}) is the entropy change, R is the universal gas constant (8.314 mol^{-1} K^{-1}), T is the absolute temperature (K), K_e is the

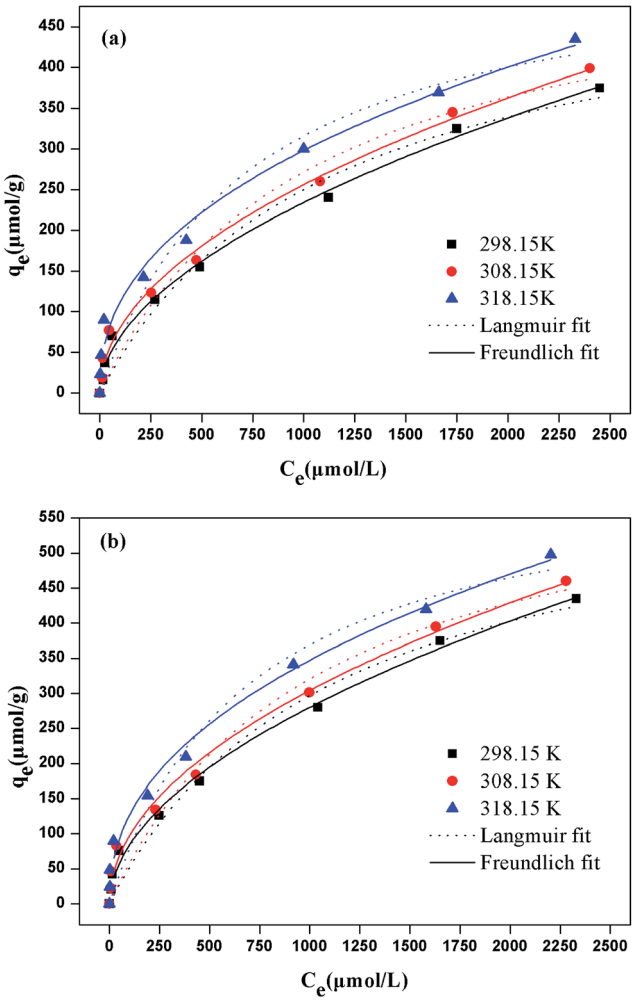

Fig. 4 Langmuir isotherm and Freundlich isotherm for the adsorption of MF on (a) 300 °C and (b) 450 °C mBC (solution volume: 50 mL; adsorbent dose: 0.1 g; contact time: 24 h; pH: 3.0).

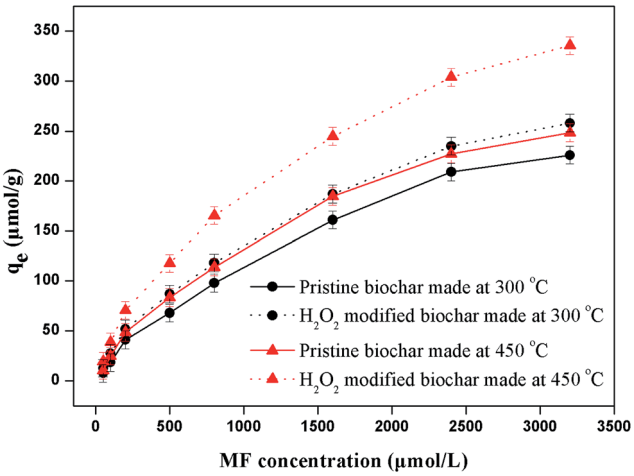

Fig. 5 The adsorption capacity of MF on BC and mBC at equilibrium (solution volume: 50 mL; adsorbent dose: 0.1 g; contact time: 24 h; pH: 7.0).

thermodynamic equilibrium constant which was calculated by plotting $\ln(q_e c_e^{-1})$ *versus* q_e and extrapolating to zero q_e. The values of ΔH^0 and ΔS^0 can be determined from the intercept and slope of the linear plot of ΔG^0 *versus* T.

Changes of temperature can affect sorption behavior of organic chemicals on sorbents. Increasing temperature can enhance the rate of molecular diffusion and decrease the viscosity of solution. Therefore, it can be easier for sorbate molecules to cross the external boundary layer and move into the internal pores of sorbents.[38] Thermodynamic parameters calculated by eqn (7) and (8) are shown in Table 5. The maximum adsorption amount of MF was obtained at 45 °C, and the maximum adsorption capacity ranged from 375 μmol g^{-1} to 435 μmol g^{-1} as the temperature ranged from 25 °C to 45 °C. The negative values of ΔG^0 at three temperatures demonstrated that the process of these adsorption were spontaneous in nature. Moreover, the more negative ΔG^0 proved that the driving force of sorption was stronger. The decrease of ΔG^0 with increasing temperature indicated that the driving force of sorption increased due to less occupation of high energy sorption sites. The positive value of ΔH^0 (7.631 kJ mol^{-1}) indicated that it is an endothermic adsorption associated with an entropy driven process ($\Delta S^0 > 0$). Furthermore, the increasing randomness at the solution/solid interface during the adsorption was proved by the positive value of ΔS^0 (33.80 J mol^{-1} K^{-1}). Therefore, the adsorption processes of MF were spontaneous and endothermic.

3.5 Adsorption of MF on biochar as affected by pH and Cu(II)

The pH is a major factor affecting adsorption of ionizable organic contaminants due to the varied species.[39] MF has

Table 4 Langmuir, Freundlich and Temkin isotherms parameters for MF sorption on mBC produced at 300 °C

		Langmuir model			Freundlich model			Temkin model		
Biochar (°C)	Temperature (K)	q_{max} (μmol g^{-1})	K_L (L μmol^{-1})	R^2	K_F (L μmol^{-1})	n	R^2	A_T (L g^{-1})	b_T	R^2
300	298.15	528.10	8.99×10^{-4}	0.97	6.03	1.89	0.99	0.05062	37.84	0.88
	308.15	551.36	9.71×10^{-4}	0.96	8.01	1.99	0.99	0.02181	40.94	0.86
450	318.15	546.10	1.37×10^{-3}	0.95	15.77	2.35	0.99	0.2126	47.81	0.85
	298.15	625.27	9.03×10^{-4}	0.97	7.50	1.92	0.99	0.08291	36.59	0.85
	308.15	648.05	9.78×10^{-4}	0.97	9.87	2.01	0.99	0.1620	41.06	0.83
	318.15	627.12	1.43×10^{-3}	0.96	16.93	2.27	0.99	0.3867	44.92	0.84

Table 5 Thermodynamic parameters for the adsorption of MF by mBC produced at 300 °C

$\ln k_e$			ΔG^0 (kJ mol^{-1})				
298.15 K	308.15 K	318.15 K	298.15 K	308.15 K	318.15 K	ΔH^0 (kJ mol^{-1})	ΔS^0 (J mol^{-1} K^{-1})
0.9858	1.089	1.176	−2.444	−2.789	−3.120	7.631	33.80

positively charged (cationic), zwitterionic, and/or negatively charged (anionic) species at different pHs due to different pk_as (pk_{a_1} = 2.97 and pk_{a_2} = 11.61).[20] The species distribution as function of pH was depicted in Fig. 6. MF molecules mainly existed as cations at pH < 2.97 and dominated as anions at pH > 11.61. In the pH range 2.97–11.61, the zwitterion was the most important species. The zero point of zeta potential (pH$_{zpc}$) was 2.6 for mBC (Fig. S2a†). When the solution pH < pH$_{zpc}$, the mBC surface contained positive charge because of the protonation of mBC's hydrated surface. Therefore, a strong electrostatic repulsion between positive charged mBC surface and cationic MF was existed, which could be responsible for the low adsorption capacity at pH < 3. However, mBC became negative charge due to the deprotonation of adsorbent's hydrated surface when pH > pH$_{zpc}$. As shown in Fig. S2b,† the adsorption capacity of MF on mBC increased with the increase of pH values at pH < 3. At pH > 3, the adsorption capacity decreased with the increase of pH values. The possible explanation may be that the amount of anions would enhance with increasing pH values at pH > 3, so the electrostatic repulsion between the surface of mBC and MF species (anions) hindered the MF adsorption.

In order to evaluate the effects of heavy metals on the adsorption of MF, Cu(II) (0.1, 0.5, and 1 mmol L^{-1}) were added into MF solution at an initial concentration of 0.5 mmol L^{-1}. The existence of Cu(II) at a low concentration could enhance the adsorption of MF onto mBC (Fig. S2c†). Moreover, a big influence of heavy metals was present at the pH 3–7, whereas the adsorption of MF in the presence of heavy metal was almost similar at pH > 7. Experiments data indicated that the adsorption capacity of MF decreased with the increase of Cu(II) concentration when the concentration of Cu(II) reached up to 0.5 and 1 mmol L^{-1}.

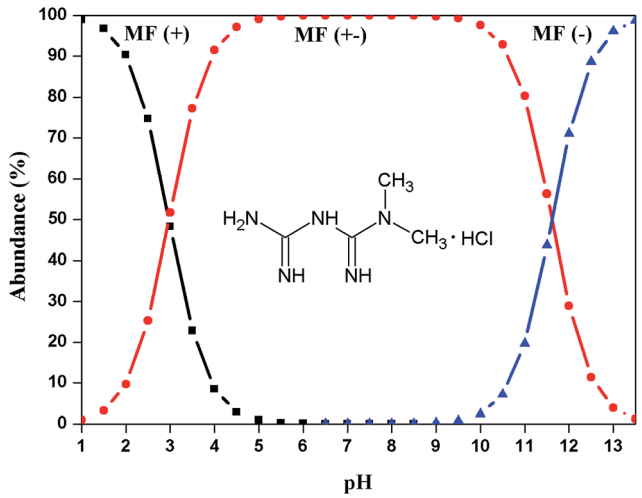

Fig. 6 Molecular structure and speciation of MF under different pH conditions.

On the one hand, the presence of Cu(II) facilitated MF adsorption on mBC at pH 3–7, which may be attributed to the formation of mono and bis-complexes of Cu(II) and MF ((Cu(MF))$^{2+}$ and (Cu(MF)$_2$)$^{2+}$), and the reduction of the mobility of MF in solution.[20] The solubility of (Cu(MF))$^{2+}$ and (Cu(MF)$_2$)$^{2+}$ were lower than those of cationic, zwitterionic and anionic of MF, showing the increasing hydrophobicity of MF in the presence of Cu(II).[20,40] The hydrophobic interactions were generally considered as an important factor for driving organic chemicals sorption on adsorbents. On the other hand, CuOH$^+$ and Cu(OH)$_2$ would form at high pH, which may be contributed to the minor effects of the presence of Cu(II) on MF adsorption by mBC at pH > 7.[23,41] Therefore, these results demonstrated that the interactions of Cu(II) and MF at different solution pH should be taken into account to understand the environmental fate.

3.6 Effect of background electrolyte on MF removal

Fig. 7 showed the effect of background electrolyte on the MF adsorption onto the mBC at pH 3 in NaCl and CaCl$_2$ (0, 0.1, 0.2, 0.4, 0.8 and 1.0 mmol L^{-1}) solution. As shown in Fig. 7, the presence of NaCl at low concentration (0.1 mmol L^{-1}) had minor effect on the adsorption capacity of MF. With the increase of NaCl concentration from 0.2 to 1.0 mmol L^{-1}, the MF adsorption capacity decreased from 114 to 97 μmol g^{-1}. However, the CaCl$_2$ could increase MF removal until the concentration of CaCl$_2$ was 0.2 mmol L^{-1}, and the adsorption capacity increased from 117 to 119 μmol g^{-1}. The effect of CaCl$_2$ on MF adsorption was sensitive when the concentration of CaCl$_2$ reached at 0.4 mmol L^{-1}. The possible explanation could be that high concentration of Na$^+$, Ca^{2+} and Cl$^-$ can hinder the electrostatic between the charges on biochar surface and MF (cationic) in solution. Moreover, Na$^+$ and Ca^{2+} could occupy surface adsorption sites of mBC firstly. In addition, the high ionic strength of the solution could influence the activity coefficient of MF, thus decreasing the contact between the sorbent and solute. The study of the effect of background electrolyte on MF adsorption indicated that electrostatic force may be one possible sorption mechanism for the removal of MF on mBC.

3.7 Regeneration and desorption analysis

Desorption properties of biochar can reflect its practical and economical value. In this study, the regeneration of mBC was conducted by using 0.5 mol L^{-1} hydrochloric acid desorption. As shown in Fig. 8, the adsorption capacity of MF decreased with the increase of cycles, but not less than 198.5 μmol g^{-1} in

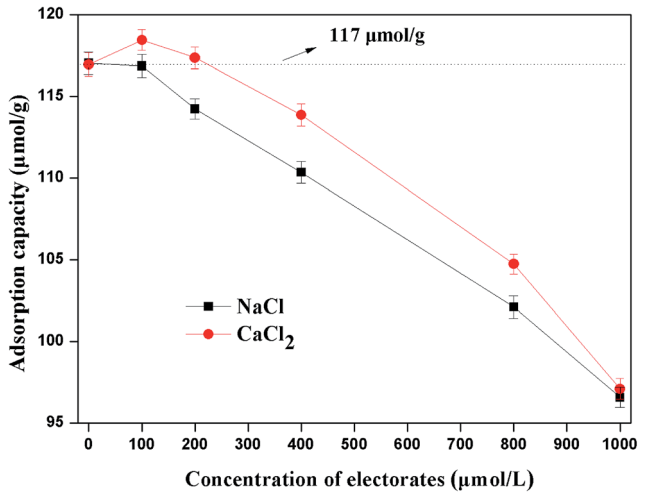

Fig. 7 Effect of background electrolyte (NaCl and $CaCl_2$) on the MF adsorption by mBC. The line of dashes indicating the adsorption capacity of MF without any interfering electrolytes (MF concentration: 0.5 mmol L^{-1}; solution volume: 50 mL; adsorbent dose: 0.1 g; contact time: 24 h; temperature: 25 °C; pH: 3.0; biochar: 300 °C).

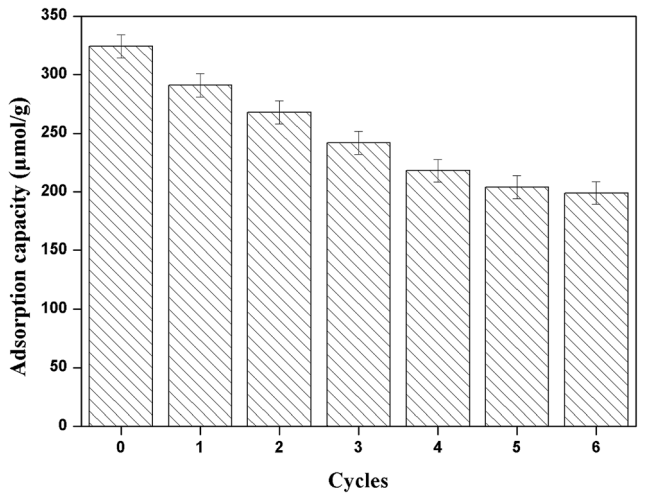

Fig. 8 Adsorption and desorption cycles of mBC for MF adsorption. (MF concentration: 2.4 mmol L^{-1}; solution volume: 50 mL; adsorbent dose: 0.1 g; contact time: 24 h; temperature: 25 °C; pH: 3.0; biochar: 300 °C).

the sixth cycle. Therefore, mBC can be regenerated by using hydrochloric acid. The reduction of specific surface area, pore volume and functional groups may contribute to the decreased adsorption capacity of MF on mBC.

4. Conclusions

This study proved that the higher temperature biochar (450 °C) and mBC had a higher adsorption capacity for MF compared to the lower temperature biochar (300 °C) and unmodified biochar. H_2O_2 treatment could increase oxygen-containing functional groups and surface area of biochar. Moreover, the adsorption mechanism was mainly attributed to the chemisorption. In addition, pH had great influence on MF adsorption by mBC and the optimum pH value was 3. The presence of Cu(II) could influence the adsorption capacity of MF at pH 3–7, which may be attributed to the formation of complexes between Cu(II) and MF. However, Cu(II) had minor effects on MF adsorption capacity at pH > 7.

Acknowledgements

This study was financially supported by the National Natural Science Foundation and Innovation Group of China (Grant no. 41271332, 51478470 and 51521006), and the Hunan Provincial Innovation Foundation For Postgraduate (Grant No. CX2015B090).

References

1 A. D. Association, *Diabetes Care*, 2010, **33**, S62–S69.
2 T. Klepser and M. Kelly, *Am. J. Health-Syst. Pharm.*, 1997, **54**, 893–903.
3 N. J. Niemuth and R. D. Klaper, *Chemosphere*, 2015a, **135**, 38–45.
4 J. Crago, C. Bui, S. Grewal and D. Schlenk, *Gen. Comp. Endocrinol.*, 2016, **232**, 185–190.
5 R. Van Aerle, T. J. Runnalls and C. R. Tyler, *J. Fish Biol.*, 2004, **64**, 335–369.
6 N. J. Niemuth, R. Jordan, J. Crago, C. Blanksma, R. Johnson and R. D. Klaper, *Environ. Toxicol. Chem.*, 2015b, **34**, 291–296.
7 M. Oosterhuis, F. Sacher and T. L. Ter Laak, *Sci. Total Environ.*, 2013, **442**, 380–388.
8 M. Scheurer, A. Michel, H. J. Brauch, W. Ruck and F. Sacher, *Water Res.*, 2012, **46**, 4790–4802.
9 A. J. Ghoshdastidar, S. Fox and A. Z. Tong, *Environ. Sci. Pollut. Res. Int.*, 2014, **22**, 689–700.
10 B. D. Blair, J. P. Crago, C. J. Hedman, R. J. F. Treguer, C. Magruder, L. S. Royer and R. D. Klaper, *Sci. Total Environ.*, 2013b, **444**, 515–521.
11 X. Tan, Y. Liu, Y. Gu, Y. Xu, G. Zeng, X. Hu, S. Liu, X. Wang, S. Liu and J. Li, *Bioresour. Technol.*, 2016, **212**, 318–333.
12 X. Tan, Y. Liu, G. Zeng, X. Wang, X. Hu, Y. Gu and Z. Yang, *Chemosphere*, 2015, **125**, 70–85.
13 X. Chen, G. Chen, L. Chen, Y. Chen, J. Lehmann, M. B. McBride and A. G. Hay, *Bioresour. Technol.*, 2011, **102**, 8877–8884.
14 W. K. Kim, T. Shim, Y. S. Kim, S. Hyun, C. Ryu, Y. K. Park and J. Jung, *Bioresour. Technol.*, 2013, **138**, 266–270.
15 M. Ahmad, S. S. Lee, X. Dou, D. Mohan, J. K. Sung, J. E. Yang and Y. S. Ok, *Bioresour. Technol.*, 2012, **118**, 536–544.
16 B. Chen, Z. Chen and S. Lv, *Bioresour. Technol.*, 2011, **102**, 716–723.
17 B. Qin, *Ecol. Eng.*, 2009, **35**, 1569–1573.
18 L. Xiao, L. Ynag, Y. Zhang, Y. Gu, L. Jiang and B. Qin, *Ecol. Eng.*, 2009, **35**, 1668–1676.
19 M. M. Correia dos Santos, V. Famila and M. L. Simoes Goncalves, *Anal. Biochem.*, 2002, **303**, 111–119.
20 S. R. Devi, *Int. J. Enginee. Sci. Inven.*, 2013, **2**, 39–50.

21 G. Wilkinsion, R. D. Gillard and J. A. McCleverty, *Comprehensive Coordination Chemistry*, Oxford, Pergamen, 1987.
22 T. X. Bui and H. Choi, *Chemosphere*, 2010, **80**, 681–686.
23 Y. J. Wang, D. A. Jia, R. J. Sun, H. W. Zhu and D. M. Zhou, *Environ. Sci. Technol.*, 2008, **42**, 3254–3259.
24 Z. Zhang, K. Sun, B. Gao, G. Zhang, X. Liu and Y. Zhao, *J. Hazard. Mater.*, 2011, **190**, 856–862.
25 S. Stankovich, D. A. Dikin, R. D. Piner, K. A. Kohlhaas, A. Kleinhammes, Y. Jia, Y. Wu, S. T. Nguyen and R. S. Ruoff, *Carbon*, 2007, **45**, 1558–1565.
26 L. Tang, G. D. Yang, G. M. Zeng, Y. Cai, S. S. Li, Y. Y. Zhou, Y. Pang, Y. Y. Liu, Y. Zhang and B. Luna, *Chem. Eng. J.*, 2014, **239**, 114–122.
27 D. D. Das, M. I. Schnitzer, C. M. Monreal and P. Mayer, *Bioresour. Technol.*, 2009, **100**, 6524–6532.
28 T. Y. Jiang, J. Jiang, R. K. Xu and Z. Li, *Chemosphere*, 2012, **89**, 249–256.
29 C. Moreno-Castilla, M. A. Ferro-Garcia, J. P. Joly, I. Bautista-Toledo, F. Carrasco-Marin and J. Rivera-Utrilla, *Langmuir*, 1995, **11**, 4386–4392.
30 M. B. Ahmed, J. L. Zhou, H. H. Ngo, W. Guo and M. Chen, *Bioresour. Technol.*, 2016, **214**, 836–851.
31 Y. S. Ho and G. McKay, *Process Biochem.*, 1999, **34**, 451–465.
32 Y. Sun, Q. Yue, B. Gao, Y. Gao, X. Xu, Q. Li and Y. Wang, *J. Taiwan Inst. Chem. Eng.*, 2014, **45**, 681–688.
33 J. Febrianto, A. N. Kosasih, J. Sunarso, Y. H. Ju, N. Indraswati and S. Ismadji, *J. Hazard. Mater.*, 2009, **162**, 616–645.
34 S. Sen Gupta and K. G. Bhattacharyya, *Adv. Colloid Interface Sci.*, 2011, **162**, 39–58.
35 W. Liu, J. Zhang, C. Zhang and L. Ren, *Chem. Eng. J.*, 2011, **171**, 431–438.
36 M. J. Ahmed and S. K. Theydan, *Powder Technol.*, 2012, **229**, 237–245.
37 K. Foo and B. Hameed, *Chem. Eng. J.*, 2010, **156**, 2–10.
38 Z. Y. Wang, X. D. Yu, B. Pan and B. S. Xing, *Environ. Sci. Technol.*, 2010, **44**, 978–984.
39 D. Zhang, B. Pan, H. Zhang, P. Ning and B. S. Xing, *Environ. Sci. Technol.*, 2010, **44**, 3805–3811.
40 H. Li, D. Zhang, X. Han and B. Xing, *Chemosphere*, 2014, **95**, 150–155.
41 D. A. Jia, D. M. Zhou, Y. J. Wang, H. W. Zhu and J. L. Chen, *Geoderma*, 2008, **146**, 224–230.

